Desalination and Water Treatment
www.deswater.com
doi: 10.1080/19443994.2014.950995

56 (2015) 1507–1519
November

Taylor & Francis
Taylor & Francis Group

Remediation of Eriochrome Black T-contaminated aqueous solutions utilizing H_3PO_4-modified berry leaves as a non-conventional adsorbent

M. Ahmaruzzaman*, Md. Juned K. Ahmed, Shamima Begum

Department of Chemistry, National Institute of Technology Silchar, Silchar 788010, India, Tel. +91 9435522348; Fax: +91 3842224797; email: md_a2002@rediffmail.com (M. Ahmaruzzaman), Tel. +91 9678170176; email: juned.nits@gmail.com (Md.J.K. Ahmed), Tel. +91 8822810253; email: shami.bm11@gmail.com (S. Begum)

Received 25 February 2014; Accepted 4 July 2014

ABSTRACT

The present investigation addresses the feasibility study of H_3PO_4-modified berry leaves (HMBL) towards the abatement of Eriochrome Black T (EBT) from aqueous solutions. The adsorbent is characterized by functional groups like hydroxyl, primary amine NH bending, aromatic phosphate (P–O–C stretch) and CH bending of alkyne group; BET surface area of 824.98 $m^2\ g^{-1}$ and homogenous surface morphology. Retention of EBT in batch system was executed to optimize the influencing variables for better adsorptive performance. The dye uptake reached equilibrium at 1 h with an optimum adsorbent load of 2 $g\ L^{-1}$ under optimum temperature of 303 K. Equilibrium adsorption isotherm data were in good agreement (R^2 = 0.996) to Langmuir isotherm with monolayer adsorption capacity of 133.33 $mg\ g^{-1}$ at 303 K. The adsorption process followed pseudo-second-order kinetics with higher R^2 (0.9999) and lesser $\Delta q\%$ (0.439). Thermodynamic investigation revealed the adsorption process to be exothermic ($\Delta H = -37.149$ kJmol^{-1}) and spontaneous in nature ($\Delta G = -5.937$ kJmol^{-1} at 303 K) with a decrease in the randomness ($\Delta S = -103.01\ J\ K^{-1}\ mol^{-1}$) at the solid/liquid interface. The exhausted HMBL can be regenerated by 0.1 M NaOH and utilized for three adsorption–desorption cycles. The estimated cost of HMBL (USD 10.684/kg) is less as compared to commercial activated carbon (CAC) (USD 172.96/kg). The results implied the promising candidature of HMBL as a non-conventional low-cost alternative to CAC for dye removal.

Keywords: Adsorption; Modified berry leaves; Eriochrome Black T; Kinetics; Thermodynamics

1. Introduction

Widespread use of synthetic dyes like azo dyes is anticipated in textile, paper, plastic, rubber, cosmetics, pharmaceutical and food industries because of their ease of use, inexpensive cost of synthesis, stability and variety of colour compared to natural dyes. Wastewaters from these industries represent a serious problem all over the world as most of the dyes are difficult to biodegrade due to their complex aromatic molecular structure and synthetic origin. It is estimated that during the dyeing process 1–15% of the dye is lost in the effluents [1]. Most of these dyes are toxic, mutagenic and carcinogenic in nature and are very stable to light and oxidizing agents, which makes them refractory compounds [2]. The extensive use of dyes often causes pollution problems in the form of coloured wastewater discharged into environmental water bodies and cause threat to aquatic life. Dyes in aqueous streams

*Corresponding author.

make penetration of sunlight difficult to reach the lower water layers, consequently, affecting photosynthesis [3] of aquatic plants. Thus, the remediation of dye-contaminated aqueous streams is of utmost concern for environmental sanitation.

Various physico-chemical methods are attempted for the treatment of dye-contaminated streams such as adsorption, ion-exchange, chemical oxidation, biodegradation, coagulation, flocculation, precipitation, membrane separation, reverse osmosis and electrochemical methods [4]. Among these, adsorption is the noteworthy procedure of choice because of its effectiveness in dye removal. It has been proved by many researchers that removal of dyes by activated carbon is favourable and technically easier.

Activated carbon is widely used as an adsorbent due to its high adsorption capacity, high surface area, microporous structure and high degree of surface but its use is usually limited due to its high cost. In order to decrease the cost of treatment, attempts have been made to find inexpensive alternative adsorbents and to serve the purpose natural agro-based wastes are a good choice. The production of activated carbon from these sources may reduce the cost of wastewater treatment and at the same time open new market for low-cost agricultural by-product. A number of non-conventional, low cost biomass such as coconut coir [5], banana pith, maize cob [6], pineapple stem [7], jute fibre [8], palm fibre [9], coconut shells, groundnut shell, bamboo dust [10], acorn shell [11,12], almond shell [13], pistachio shell [14], cotton waste [15,16], maize stem [17], mosambi peel [18] and nilgiri leaves [19] have been utilized for the production of activated carbon and tested for the removal of different dyes from aqueous solutions at different operating conditions. Waste materials like wheat husk [20] and hen feathers [21] are also utilized for treating hazardous dye-contaminated wastewater [22,23]. Alternative to commercial activated carbon (CAC), low-cost adsorbents are nowadays developed from industrial waste materials like bottom ash and de-oiled soya [24–29], bagasse fly ash [30], waste rubber tire [31], blast furnace slag, dust, sludge and carbon slurry [32–34] for the removal of dyes, metals and various organic compounds from aqueous streams. The use of biosorbents [35] and expensive adsorbents viz. carbon nanotubes [36,37], TiO_2 catalyst [38] are also utilized for the removal of toxic entity(s) [39] from aqueous solutions. However, on extensive literature study, it is observed that there are no reports available on the exploration of the adsorption potential of agro-based waste like berry leaves for the removal of Eriochrome Black T (EBT) from aqueous phase. So, in the present study, berry leaves are selected as the precursor for the development of low-cost adsorbent.

The objective of the present study is focused on the development of non-conventional adsorbent from the precursor materials (berry leaves) by chemical activation with H_3PO_4 and thereby, exploring the potential and feasibility of the developed adsorbent for the remediation of EBT-contaminated aqueous solutions. The cost associated with the development of the adsorbent is also evaluated to justify its applicability in the ground of economic consideration.

2. Materials and methods

2.1. Materials

The model anionic azo dye EBT was procured from Merck India and synthetic stock solution (1,000 mg L^{-1}) of EBT was prepared in double distilled water (DDW). The stock solutions were diluted to obtain test solution of required concentration. All the chemicals and reagents used in the experimental studies were of analytical grade. Berry leaves were collected within NIT Silchar campus.

2.2. Adsorbent development

The biomass (berry leaves) was repeatedly washed with DDW to remove adhered dirt/impurities and dried in an oven at 383 K for 5 h. The treated biomass was chemically impregnated (impregnation ratio = 2.0) using H_3PO_4 at 373 K for 20 min on a hot plate followed by carbonization at 773 K in a muffle furnace (heating rate = 273 K min^{-1}) under N_2 atmosphere (flow rate = 100 cm^3 min^{-1}) for 1 h. In this regard, it needs to be mentioned that an inert atmosphere is maintained so as to avoid the combustion of carbonaceous matter and higher impregnation ratio is restricted as it has a negative effect on the carbon yield% [5]. The method of chemical activation was adopted to enhance porosity development besides carbonizing the leafy biomass. During the acid treatment, the biomass is digested to form a black carbonaceous paste. This paste on carbonization in muffle furnace resulted in the development of several porous structure due to the evaporation of H_3PO_4 leaving behind the space formerly occupied by the acid molecules. The carbonized material was washed repeatedly with DDW to remove any free acids that may be present on the adsorbent surface until a pH of ~7. The final product was then kept in an oven at 383 K for 6 h to remove the excess moisture trapped inside the pores of the adsorbent. The adsorbent was finely ground and stored in an air-tight container prior to its use in

adsorption. The adsorbent, thus, developed is referred to as H_3PO_4-modified berry leaves (HMBL).

2.3. Adsorbent characterization

The physical and chemical analysis of HMBL was conducted according to American Standard for Testing and Materials (ASTM) standard. Proximate analysis or Macro analysis (ASTM D-3172) of the adsorbent constitutes determination of moisture, volatile matter, ash content and fixed carbon content as wt.% (as received) using a hot air oven and a muffle furnace. Ultimate analysis or Micro analysis (ASTM D-3176) includes determination of carbon, hydrogen and nitrogen content as wt.% (dry ash free basis) which was done by a Thermo Finnigan FLASH EA 1112 series CHNS(O) Analyser. To understand the morphology, a scanning electron microscope ([SEM] Leo 1430 VP) was used. The sample was first gold coated using sputter coater (Edwards S150) which provides conductivity to the sample, and then the SEM images were recorded. FT-IR analysis of the HMBL samples was performed on a Nicolet MAGNA-550 FTIR spectrophotometer to study the functional groups on the adsorbent surface. Powdered sample was first dried at 383 K for 24 h and then the dried sample was mixed with finely divided KBr at a ratio of 1:300. A FTIR spectrum was recorded at a resolution of 4 cm^{-1} and with 64 scans per sample and an aperture setting of 15 Å. A previously recorded background spectrum of water vapour was subtracted from the spectrum of the sample. Textural characteristic of the adsorbent was determined by nitrogen adsorption at 77.71 K using a Micromeritics, ASAP 2010 Surface Area Analyzer. The adsorption/desorption isotherms are used to find out the Brunauer–Emmett–Teller (BET) surface area, pore volume and pore size distribution. The samples were first out-gassed at 473 K for at least 4 h under vacuum. Barret–Joyner–Halenda (BJH) desorption method was used to calculate the average pore diameter and cumulative volume of the pores while the specific surface area was evaluated from the N_2 adsorption isotherms by applying the Brunauer et al. equation [40] in the relative pressure (P/P_0) range.

2.4. Adsorption assay

Batch equilibrium studies were carried out to find the optimum adsorbent load, contact time, effect of temperature and initial concentration. The kinetics and thermodynamics of adsorption, modelling of isotherm data for the adsorption of EBT onto HMBL were also explored. The retention of EBT in batch system was conducted by agitating known amount of the adsorbent (0.01–0.08 g) with 25 mL of EBT solution (200 mg L^{-1}). The solution containing the adsorbent was filtered using Whatmann filter paper no. 42 or it was centrifuged in case of low adsorbent dose. Thus, the optimum amounts of adsorbents required for the removal of EBT were obtained. For contact time dependent characteristics, optimum amounts of the adsorbents were taken in several Erlenmeyer flasks containing 25 mL of EBT solution (200 mg L^{-1}) for different contact time at 303 K. For temperature dependent characteristics, the same process is followed but stirred for optimum contact time and at different temperatures (303, 313 and 323 K). In all the above analyses, the amount of EBT adsorbed at equilibrium was calculated by the mass balance equation given by Eq. (1):

$$q_e = \frac{(C_0 - C_e) \times V}{m \times 1,000} \tag{1}$$

The percentage removal of EBT from solution was calculated by Eq. (2):

$$\% \text{ Removal} = \frac{(C_0 - C_e)}{C_0} \times 100 \tag{2}$$

where q_e (mg g^{-1}) is the quantity of the adsorbate per unit mass of the adsorbent at equilibrium, V (mL) is the volume of the adsorbate, C_0 (mg L^{-1}) is the initial liquid phase adsorbate concentration, C_e (mg L^{-1}) is the equilibrium liquid phase concentration and m (g) is the mass of HMBL.

2.5. Kinetic investigation

The equilibrium adsorption time for the uptake of EBT by HMBL was estimated through kinetic studies. The kinetic experiments were conducted at 303 K in a standardized batch experimental set up which comprised of several 100 mL stoppered Erlenmeyer flasks containing EBT solutions (25 mL each) kept in contact with 0.04 g of HMBL placed inside the incubator cum shaker maintained at a controlled speed of 140 rpm for different contact time. At the end of the predetermined time t, the flasks were withdrawn and their contents filtered/centrifuged, and measured for residual EBT concentration by UV–visible spectrophotometer. The adsorption kinetics was followed for 1 h. The kinetics of adsorption of EBT was investigated using various kinetic models, viz. pseudo-first-order and pseudo-second-order model and validated by normalized standard deviation.

2.6. Adsorption isotherm

The experimental adsorption data were investigated using Langmuir and Freundlich models to govern the best model that characterizes the adsorption mechanism. The Langmuir model [41] is based on the assumption of monolayer, uniform adsorption, with finite number of active sites and with no lateral interaction and steric hindrance between the adsorbed molecules (even on the adjacent sites). The linearized form of Langmuir isotherm can be expressed as:

$$\frac{C_e}{q_e} = \frac{1}{ab} + \frac{C_e}{a} \quad (3)$$

where C_e is the equilibrium concentration of the adsorbate in solution after adsorption (mg L^{-1}), q_e is the amount adsorbed per unit weight of adsorbent (mg g^{-1}), a and b are Langmuir constants, a depicting the monolayer adsorption capacity. A linear plot of C_e/q_e vs. C_e gives the value of a (mg g^{-1}) and b (L g^{-1}) from the slope and intercept, respectively.

The Freundlich model [42] is an empirical model relating to multilayer adsorption, with non-uniform distribution of adsorption heat and affinities over the heterogeneous surface of the adsorbent. The linearized expression of the Freundlich isotherm is:

$$\log q_e = \log k_F + 1/n \log C_e \quad (4)$$

where k_F (mg g^{-1}) (L $mg^{-1})^{1/n}$ is the Freundlich equilibrium constant which is an indication of adsorption capacity and $1/n$ is an empirical constant related to the efficiency of adsorption: if $1/n > 1$, the adsorption is unfavourable, while $1/n < 1$, indicates favourable adsorption.

3. Results and discussion

3.1. Characterization of HMBL

A result of physico-chemical analysis of HMBL is given in Table 1. The fixed carbon content was comparatively high and found to be 55.75%. Ultimate analysis showed the carbon content of HMBL as 50.62% which is comparable to the proximate analysis result. The high carbon content and low moisture content can be attributing to facilitate the adsorption of EBT on HMBL surface.

The SEM images revealed the characteristic surface morphology of the adsorbent. Fig. 1(a) and (b) shows the SEM images of blank and EBT loaded HMBL, respectively. It is evident from the images that the blank adsorbent samples of HMBL depict a highly homogenous surface (regularity in surface morphology) with uniformly oriented pits of several sizes along with some flaky particles. The development of several porous structures is also observed that may be attributed to the chemical activation process with phosphoric acid. This development of porous structure along with surface roughness is parallel to the increase in surface area of the adsorbent facilitating the adsorption phenomenon. The SEM images (post-adsorption of EBT) revealed a decrease in the surface roughness/porosity of the adsorbent which may be ascribed to the surface coverage of HMBL by EBT molecules indicating the adsorption of EBT.

The FTIR spectra of blank and EBT-loaded HMBL (Fig. 2) gives an insight into the functional groups present on the surface of the adsorbent and their interaction with EBT during the adsorption process. The spectra exhibit typical adsorption bands, which can be assigned to certain functional groups. The broad peak at 3,424 cm^{-1} is the characteristic peak of the hydroxyl group, and the shifting of the peak from 3,424 to 3,421 cm^{-1} can explain the involvement of H-bonded OH stretch in the adsorption of EBT on

Table 1
Physico-chemical characteristics of HMBL

Proximate analysis or macro analysis (wt.% as received)	Values
Moisture	2.08
Volatile matter	27.60
Ash	14.57
Fixed carbon	55.75
Ultimate analysis or micro analysis (wt.% dry ash free basis)	
Carbon	50.62
Hydrogen	2.35
Nitrogen	2.55
Sulphur	0
Oxygen (remaining)	44.48
Textural characteristics	
Surface area of pores (m^2 g^{-1})	
Single point	821.18
(i) BET	824.98
(ii) BJH	
(a) Adsorption cumulative	327.26
(b) Desorption cumulative	440.34
Single point adsorption total pore volume (cm g^{-1})	0.68
Average pore diameter (nm)	
(i) BET	3.31
(ii) BJH adsorption	7.04
(iii) BJH desorption	5.69

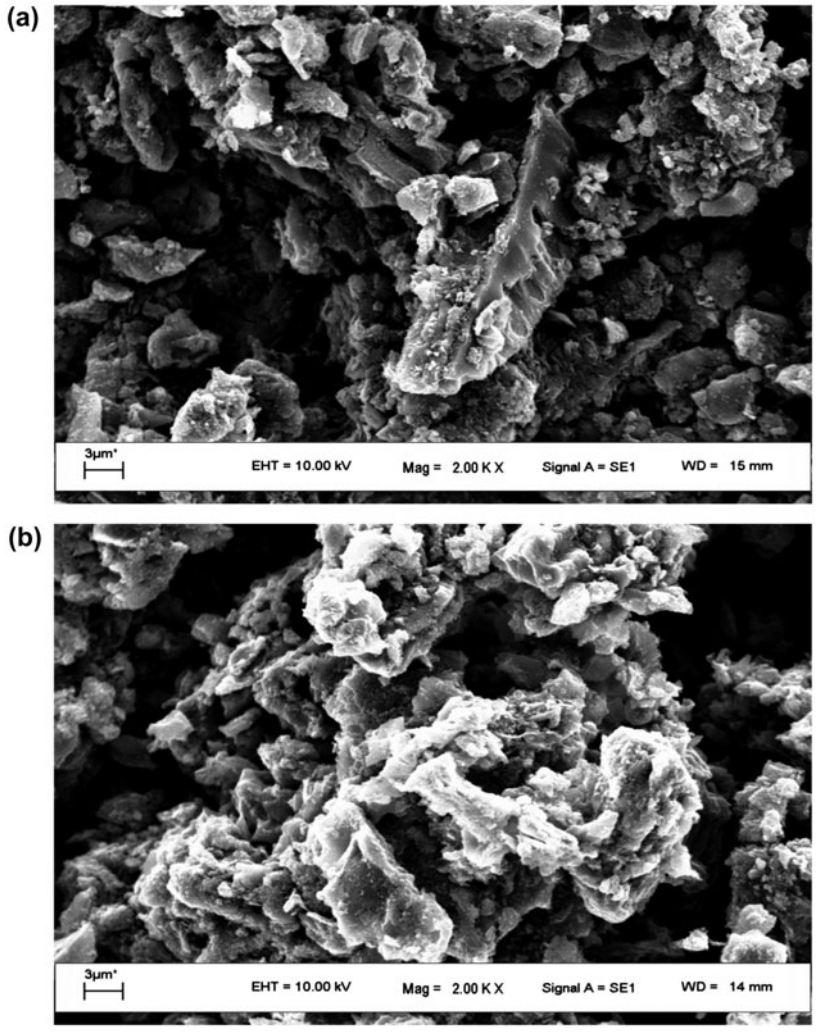

Fig. 1. SEM images of (a) blank and (b) EBT loaded HMBL at 2.00 KX magnification.

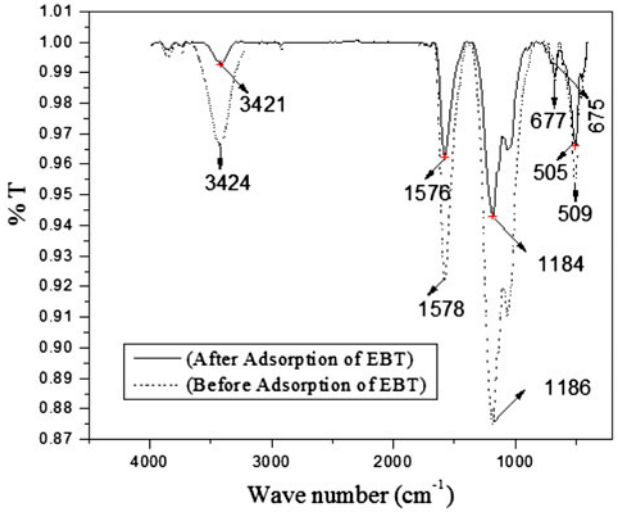

Fig. 2. FTIR spectra of blank and EBT loaded HMBL.

HMBL. The clear peak at 1,578 cm^{-1} which may be assigned to primary amine NH bending seemed to be affected by EBT adsorption and shifts to 1,576 cm^{-1}. The presence of this peak is further supported by the nitrogen content as reported in the ultimate analysis of HMBL. The peak at 1,186 cm^{-1} which shifts to 1,184 cm^{-1} after adsorption corresponds to aromatic phosphate (P–O–C stretch) which is an indication of the introduction of phosphate on the adsorbent surface as a result of phosphoric acid activation of berry leaves. Alkyne C–H bending is apparent from the small peak at around 677 cm^{-1} which shifts to 675 cm^{-1} after adsorption of EBT on HMBL. Thus, the functional groups that can be held responsible for the adsorption of EBT on HMBL are: (i) hydroxyl group (–OH stretch), (ii) primary amine NH bending, (iii) aromatic phosphate (P–O–C stretch) and (iv) CH bending of alkyne group.

A good adsorbent is characterized by their high porosity and larger surface area with more specific adsorption sites [43,44]. The specific surface area of HMBL was calculated from nitrogen adsorption data according to BET model. Table 1 shows the BET, BJH surface area analysis and pore volume distribution of HMBL. The BET surface area of HMBL was found 824.98 $m^2\ g^{-1}$ which is almost comparable to the single-point surface area (821.18 $m^2\ g^{-1}$). The N_2 adsorption and desorption isotherm plot of HMBL (Fig. 3) showed that the isotherm belong to Type II as defined by IUPAC classification [45,46]. The pore structure is also a major factor affecting the adsorption process. If the pore diameter is such that the adsorbate molecules are larger, then lesser adsorption would take place due to steric hindrance. According to the IUPAC classification of pore dimensions, there are three broad classifications grouped as: micropore (≤2 nm), mesopore (2–50 nm) and macropore (≥50 nm). The standard BJH method [47] was used to calculate the pore size distribution curve of HMBL during adsorption and desorption. The single-point adsorption total pore volume of pores less than 73.19 nm diameter at P/P_0 of 0.97 was found 0.683 $cm^3\ g^{-1}$ which showed the microporous nature of the adsorbent. The average pore diameter of HMBL as determined by BET method was 3.31 nm indicating a very narrow pore size distribution in the mesoporous range. The fraction of pores opened at both ends was found to be nil. The BJH adsorption pore distribution plot (figure not shown) revealed that the maximum concentration of the pores lies in the diameter range of 1–15 nm with average diameter of 3.31 nm. Thus, it is evident that the largest contribution to the total pore volume is contributed by the mesopores followed by certain number of micropore.

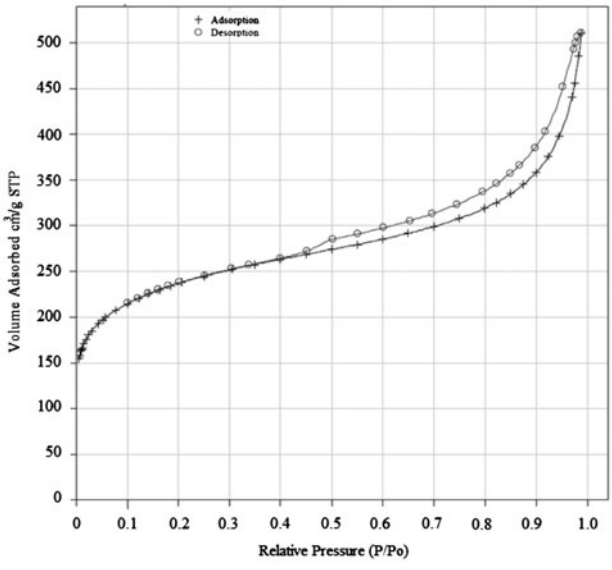

Fig. 3. N_2 adsorption–desorption isotherm plot of HMBL.

3.2. Effect of influencing parameters on the remediation of EBT

The influence of adsorbent load on the removal of dye was explored by varying the dose of adsorbent, with initial dye concentration of 200 mg L^{-1}, fixed contact time of 1 h, at 303 K and under natural pH. As shown in Fig. 4(a), the percentage uptake of EBT increases with increasing adsorbent load of HMBL. This increase in the percent removal of dye with the increase in adsorbent load is due to the availability of larger surface area with more active functional groups [48]. The adsorption of EBT increases from 56.03 to 92.03% when adsorbent load increased from 0.4 to 2.0 g L^{-1}. Further no significant improvement in adsorption with respect to the high adsorbent loading was observed. It could be explained as a consequence of a partial aggregation of EBT, which results in a decrease in effective surface area available for adsorption. So an optimum load of 2 g L^{-1} of HMBL shows maximum adsorption for EBT removal from aqueous solutions.

The effect of contact time on EBT adsorption was executed with the optimum adsorbent load of 2 g L^{-1} at 303 K for different periods of contact time with the maximum contact time of 4 h. Fig. 4(b) illustrates the %removal of EBT as a function of time. The figure depicts that the adsorption profile reaches saturation within 1 h indicating the attainment of equilibrium. Adsorption was rapid within the first 1/2 h and became almost asymptotic after 1.5 h. The decrease of adsorption rates is well illustrated by the plateau line after 1 h of adsorption. The rapid uptake of EBT during the first 1/2 h can be ascribed to the bulk diffusion of EBT molecules from the solution phase to the solid surface of the adsorbent due to concentration gradients. Thereafter, it slows down as this concentration gradient is reduced due to the accumulation of EBT molecules on the HMBL surfaces, and the adsorption reaches its equilibrium where the adsorption rate equals the desorption rate.

The impact of initial concentration (C_0) and reaction temperature (T) on the equilibrium uptake of EBT by HMBL at m = 2 g L^{-1} and t = 1 h was studied. A plot of percent removal vs. C_0 with temperature (303, 313 and 323 K) as a parameter is shown in Fig. 4(c). It is obvious that the percent removal of EBT from the solution decreases with an increase in C_0 and

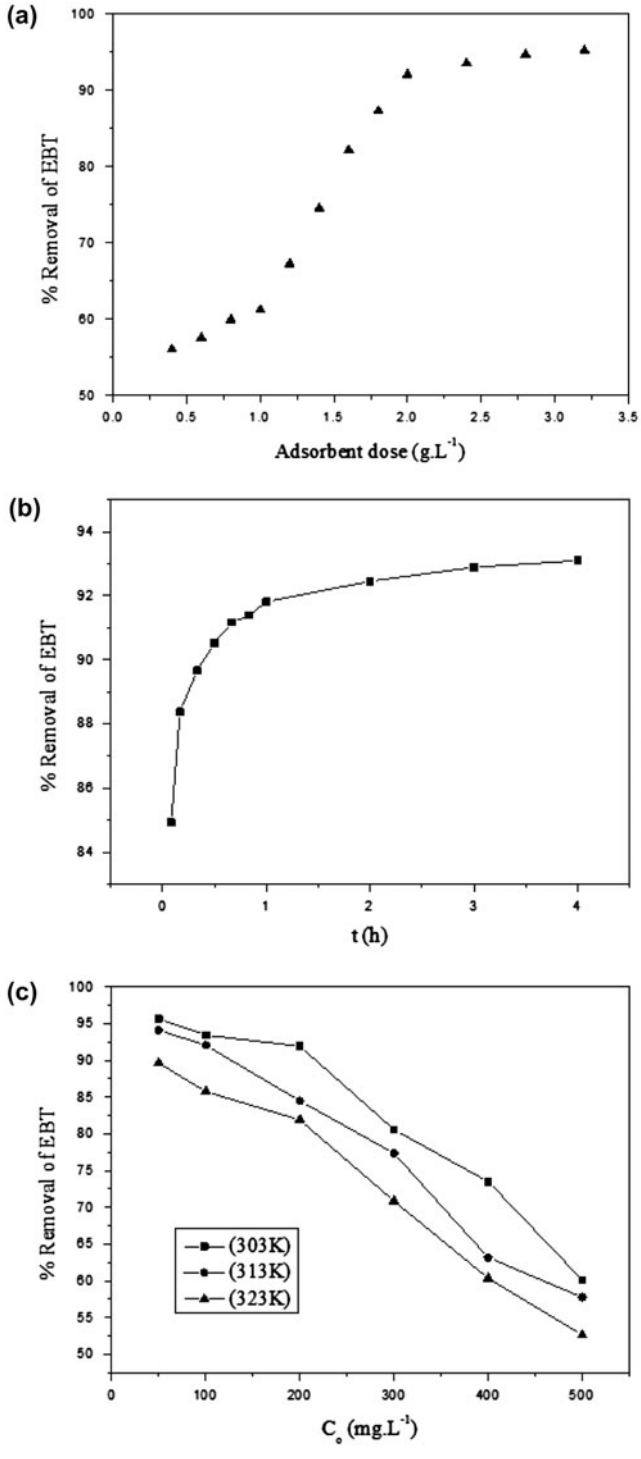

Fig. 4. Effect of influencing parameters on adsorption of EBT by HMBL (a) effect of adsorbent load (m); C_0 = 200 mg L^{-1}, t = 1 h, T = 303 K, (b) influence of contact time (t); C_0 = 200 mg L^{-1}, m = 2 g L^{-1}, T = 303 K, and (c) effect of initial concentration (C_0) and reaction temperature (T); m = 2 g L^{-1}, t = 1 h.

temperature. EBT removal is about 96% at low C_0 (50 mg L^{-1}) and more than 60% at the highest C_0 (500 mg L^{-1}) and at the lowest temperature (303 K). The increase in temperature from 303 to 323 K leads to the decrease in adsorption confirming the exothermic nature of adsorption. However, with the increase in initial concentration of EBT, the adsorptive uptake was observed to be fast due to greater driving force owing to concentration gradient between the surface of the adsorbent and the bulk of the solution.

3.3. Adsorption kinetics

The kinetic data of EBT removal by HMBL were analyzed using pseudo-first-order model (Eq. (5)), pseudo-second-order model (Eq. (6)) and validated by the normalized standard deviation (Eq. (7)). The pseudo-first-order equation [49] is given by:

$$\log(q_e - q_t) = \log q_e - \frac{k_1 t}{2.303} \tag{5}$$

The pseudo-second-order equation [49] is expressed as:

$$\frac{t}{q_t} = \frac{1}{K_2 q_e^2} + \frac{t}{q_e} \tag{6}$$

where q_e is the adsorption capacity at equilibrium (mg g^{-1}), q_t is the adsorption capacity at time t (mg g^{-1}), k_1 is the rate constant of the pseudo-first-order equation (h^{-1}); and k_2 is the pseudo-second-order rate constant (g mg^{-1} h^{-1}).

A plot of log ($q_e - q_t$) against t (Fig. 5(a)) should give a linear relationship with the slope of (k_1/2.303) and intercept of log q_e for pseudo-first-order model and a linear relationship for the plot of t/q_t against t (Fig. 5(b)) for pseudo-second-order model. The slope and intercept of the corresponding plot gives the values for q_e and k_2. The kinetic parameters for both the reported models are presented in Table 2 which shows a good agreement between the experimental and the calculated q_e value from the pseudo-second-order rate equation. Besides, the coefficient of determination (R^2) for the pseudo-second-order kinetic model approaches 1 (0.9999) in comparison to pseudo-first-order model (R^2 = 0.991), indicating better applicability of the pseudo-second-order model. Thus, it can be concluded that adsorption of EBT onto HMBL follows pseudo-second-order kinetics.

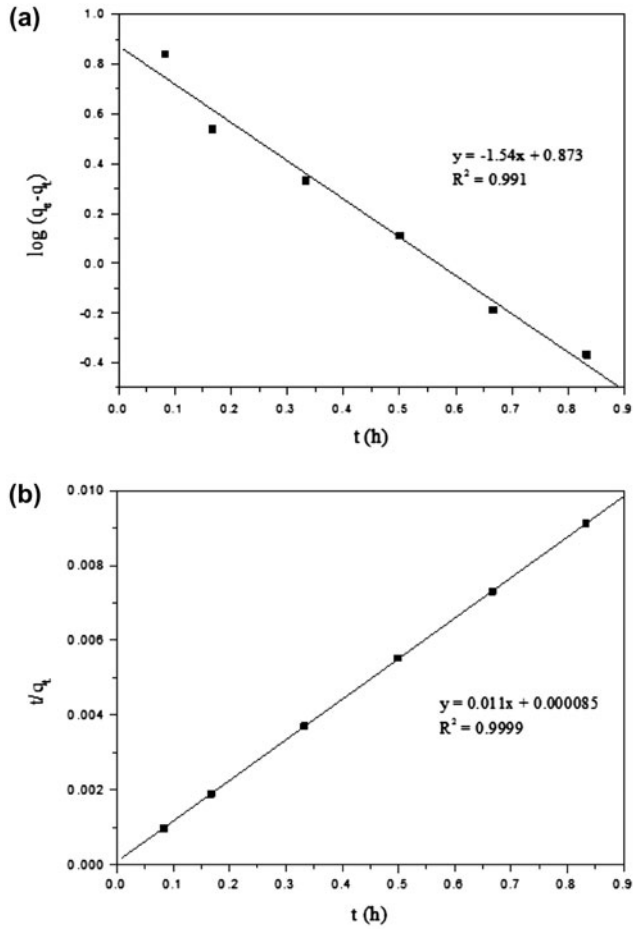

Fig. 5. Kinetics plot for EBT adsorption onto HMBL; C_0 = 200 mg L^{-1}, m = 2 g L^{-1}, T = 303 K, (a) pseudo-first-order kinetics, and (b) pseudo-second-order kinetics.

3.3.1. Validity of kinetic model

The applicability of the kinetic model to define the adsorption process was further validated by the normalized standard deviation, $\Delta q\%$, which is defined as [50]:

$$\Delta q(\%) = 100\sqrt{\frac{\sum\left[\left(q_{exp} - q_{cal}\right)/q_{exp}\right]^2}{(N-1)}} \quad (7)$$

where N is the number of data points and q_{exp} and q_{cal} (mg g^{-1}) are the experimental and the calculated adsorption capacities, respectively. Table 2 list the Δq (%) values obtained for the two models tested. It is evident from the table that the adsorption of EBT onto HMBL follows pseudo-second-order kinetics as the value of Δq (%) <1.

3.4. Adsorption isotherm modelling

The investigation on adsorption isotherm was conducted by fitting the data on Langmuir and Freundlich models. This vital step helps in determining the suitable model that characterizes the adsorption phenomena. The adsorption isotherm profile for Langmuir model and Freundlich model is illustrated in Fig. 6(a) and (b), respectively. The isotherm parameters for both the models are calculated and listed in Table 3. The linear regression co-efficient values of both the isotherm models revealed the applicability of Langmuir model (R^2 = 0.9965) in comparison to Freundlich model (R^2 = 0.9382) in describing the adsorption phenomena. The Langmuir isotherm shows an equilibrium adsorption capacity of 133.33 mg g^{-1} with monolayer coverage of EBT onto HMBL surface. The essential characteristics and feasibility of the Langmuir isotherm is further described in terms of a dimensionless parameter called the separation factor (R_L), which is defined as [50]:

$$R_L = \frac{1}{1 + bC_0} \quad (8)$$

If $0 < R_L < 1$ the adsorption process is favourable, $R_L > 1$ designates unfavourable adsorption, $R_L = 1$ denotes a linear isotherm and $R_L = 0$ indicates an irreversible adsorption. In the present study, a R_L value of 0.047 indicates the favourable adsorption of EBT onto HMBL at 303 K. The evaluation of Freundlich adsorption isotherm gives the relative adsorption capacity of the bonding energy of HMBL, k_F = 36.3 and the value of the empirical constant $1/n$ related to the efficiency of adsorption as 0.283 indicating that the favourable adsorption of EBT takes place as the value of $1/n < 1$.

Table 2
Kinetic model parameters for the adsorption of EBT onto HMBL at 303 K

C_0 (mg L^{-1})	$q_{e,exp}$ (mg g^{-1})	Pseudo-first-order kinetic model				Pseudo-second-order kinetic model			
		$q_{e,cal}$ (mg g^{-1})	k_1 (h^{-1})	R^2	Δq (%)	$q_{e,cal}$ (mg g^{-1})	k_2 (g mg^{-1} h^{-1})	R^2	Δq (%)
200	91.81	7.46	3.547	0.991	41.09	90.91	1.4	0.9999	0.439

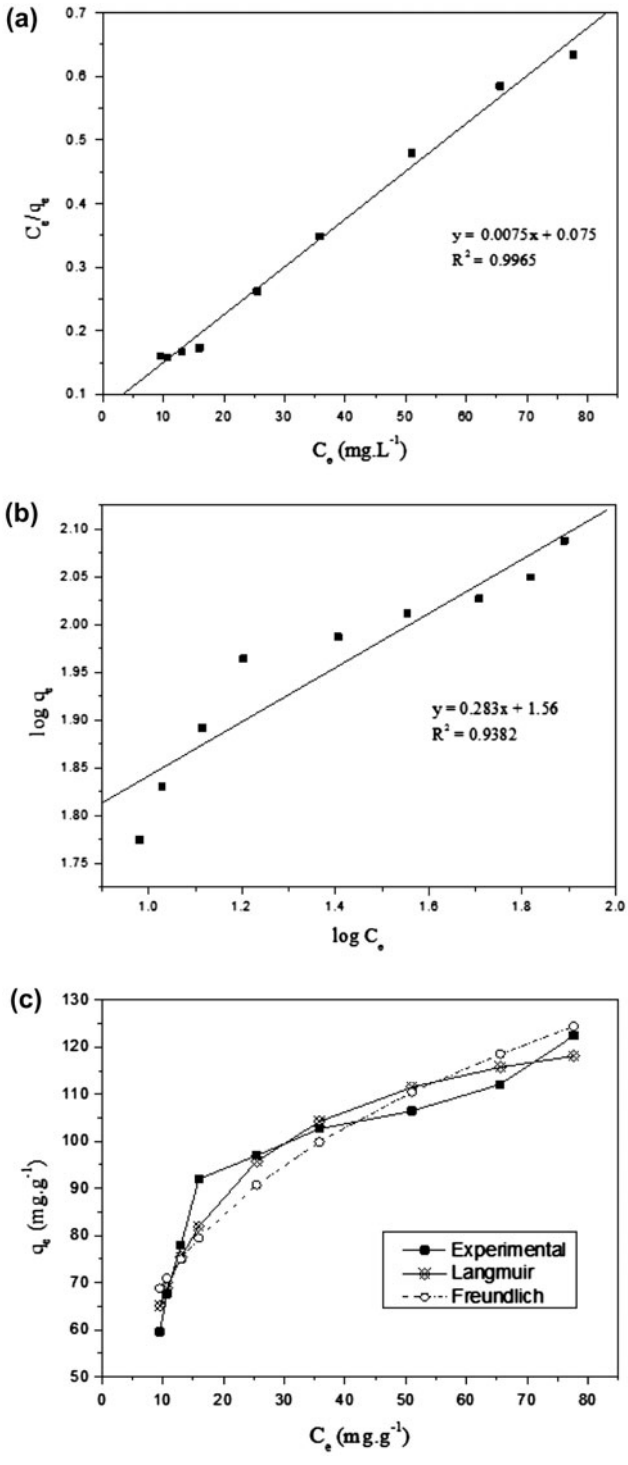

Fig. 6. Adsorption isotherm for EBT onto HMBL at 303 K; C_0 = 200 mg L^{-1}, m = 1–3.2 g L^{-1}, T = 303 K, (a) Langmuir isotherm, (b) Freundlich isotherm and (c) validity of adsorption isotherm at 303 K.

The plot in Fig. 6(c) depicts the validity of the Langmuir and Freundlich model with respect to the experimental adsorption isotherm for EBT at 303 K. The experimental adsorption isotherms follow the Type II nature of isotherm as classified by IUPAC, describing the adsorption on macroporous adsorbents with strong adsorbate-adsorbent interaction. It is evident from the figure that there is a slight deviation of Langmuir and Freundlich model from the experimental adsorption isotherm but in a comparative note Langmuir isotherm best represent the experimental findings with lesser deviation. The candidate adsorbent (HMBL) in the present study fulfils the assumption (homogenous surface morphology and monolayer coverage of adsorbate on the adsorbent surface) of Langmuir isotherm very well unlike Freundlich isotherm for heterogeneous systems. This is supported from the SEM images of blank and EBT-loaded HMBL where a uniformly homogenous surface morphology is observed before adsorption and a monolayer coverage of EBT on HMBL surface is evident post adsorption phenomena. Thus, the experimental findings from characterization and adsorption experiments completely justify the applicability of Langmuir isotherm in representing the equilibrium adsorption data.

Table 3
Isotherm parameters for the adsorption of EBT onto HMBL at 303 K

Isotherm	Parameters			R^2
Langmuir	a (mg g^{-1})	b (L g^{-1})	R_L	0.9965
	133.33	0.1	0.047	
Freundlich	$1/n_F$	k_F (mg^{-1} $L^{1/n}$ g^{-1})		0.9382
	0.283	36.3		

3.5. Adsorption thermodynamics

The effect of temperature on the adsorption of EBT by HMBL was studied in the temperature range of 303−323 K. Change in the Gibbs free energy (ΔG°) indicates the degree of the spontaneity. For significant adsorption to occur, ΔG° must be negative. The ΔG° is defined as [51]:

$$\Delta G^\circ = -RT \ln K_d \quad (9)$$

According to thermodynamics, the Gibbs free energy change is also related to the entropy change and heat of adsorption at constant temperature by the following equation [51]:

$$\Delta G^\circ = \Delta H^\circ - T\Delta S^\circ \quad (10)$$

where ΔG° is the Gibbs free energy change (kJ mol^{-1}), ΔH° is the change in enthalpy (kJ mol^{-1}), ΔS° is the entropy change (J mol^{-1} K^{-1}) and T is the absolute temperature (K).

The effect of temperature on the adsorption equilibrium constant is determined by equating Eqs. (9) and (10) which gives Eq. (11) known as van't Hoff equation:

$$\ln K_d = -\Delta H^\circ/RT + \Delta S^\circ/R \quad (11)$$

where R is the universal gas constant (8.314 J mol^{-1} K^{-1}), and $K_d = C_s/C_e$ and is called the adsorption equilibrium constant, C_e the equilibrium concentration of EBT in the solution (mg L^{-1}) and C_s is the solid phase concentration of EBT at equilibrium (mg L^{-1}). The thermodynamic parameters, ΔH° and ΔS° for the adsorption process, were obtained from slope and intercept of the plot of $\ln K_d$ vs. $1/T$ (plot not shown). Table 4 depicts the thermodynamic parameters for the adsorption of EBT by HMBL.

The exothermic nature of the adsorption process is well explained by negative value of ΔH°. In physisorption process, the adsorbate and the adsorbent are held together by weak van der Wall's force of attraction and the adsorption energy is typically 5–10 kJ mol^{-1}. In the case of chemisorption, a chemical bond exists between the adsorbate and the adsorbent having adsorption energy of 30–70 kJ mol^{-1} [52]. The adsorption of EBT onto HMBL seems to be chemisorptive in nature with ΔH° = −37.149 kJ mol^{-1}. The negative value of ΔS° (−103.01 J mol^{-1} K^{-1}) suggests decrease in the randomness of the adsorbed EBT molecules at the solid/solution interface indicating the affinity of the EBT molecules towards HMBL surface. A negative value of ΔG° signifies that the sorption process led to a decrease in Gibbs free energy with increasing temperature, thereby justifying the feasibility and spontaneity of the adsorption process.

3.6. Desorption and reusability studies with exhausted/regenerated adsorbent

The recycling and reuse is an important aspect of an adsorbent from the stand point of long-time use, industrial application and waste minimization. The exhausted EBT-loaded HMBL was regenerated using 0.1 M NaOH. For experimental run, 0.04 g of EBT-loaded HMBL was contacted with 20 mL of 0.1 M NaOH subjected to vigorous stirring (140 rpm) at 303 K for 2 h. The resultant mixture was centrifuged and the supernatant was analysed for EBT concentration. In order to establish the reusability, the regenerated adsorbent was explored for three adsorption–desorption cycles and the adsorption efficiency of each cycle was determined. Regenerated adsorbent shows dye removal efficiency of 91, 86.5 and 80.5% in successive runs in comparison to ~92% for the fresh HMBL. This shows that 98.91, 94.02 and 87.5% of the original adsorption capacity were retained by the regenerated adsorbent in three runs, respectively. Thus, the potential utilization of the adsorbent and its exploitation for industrial application is quite justified.

Table 4
Thermodynamic parameters for adsorption of EBT onto HMBL

Temperature (K)	ΔG° (kJ mol^{-1})	ΔH° (kJ mol^{-1})	ΔS° (J mol^{-1} K^{-1})
303	−5.937	−37.149	−103.01
313	−4.907		
323	−3.877		

Table 5
Cost estimation for the preparation of 1 kg of HMBL

Break up cost	Duration (h)/amount (mL)	Unit cost (USD)	Power rating (KWh)	Price (USD)
Cost of drying at oven	5	0.0664	1.5	0.498
Cost of impregnation at hot plate	0.33	0.0664	1.2	0.026
Cost of activation at furnace	1	0.0664	2.5	0.166
Cost of final drying at oven	6	0.0664	1.5	0.597
Cost of H_3PO_4 used	500	0.0168	—	8.4
Net cost				9.68
Overhead cost (10% of net cost)				0.968
Total cost				10.648

Table 6
Comparative assessment of EBT adsorption onto various non-conventional adsorbents

Adsorbent	Surface area ($m^2\ g^{-1}$)	Adsorption capacity (mg g^{-1})	References
Scolymus hispanicus L.	—	120	[2]
Cold plasma treated almond shell	—	18.18	[13]
MW radiation treated almond shell	—	29.41	[13]
Cotton stem activated carbon	198	27.1	[15]
Maize stem ground tissue	7.23	167.01	[17]
Mosambi peel activated carbon	189	46.51	[18]
Nilgiri leaves activated carbon	178	33.33	[19]
H_3PO_4-modified berry leaves	824.98	133.33	Present study

3.7. Cost evaluation of HMBL

Cost analysis is a vital parameter in establishing the criteria for utility of the adsorbent (in addition to its performance) and the choice of treatment process for environmental remediation. The utilization of waste materials to produce activated carbon for environmental remediation is of significant economic potentiality and can substitute CAC. The prepared HMBL cost USD 10.648 per kg, thereby adding economic viability in comparison to CAC (Merck, Charcoal activated, pure) which comes at a market value of USD 172.96 per kg. Table 5 shows the breakup cost estimation [53] of HMBL used in the present study. Due to the local availability of the agricultural waste, the transportation cost is negligible. The cost of storage is also eliminated as the adsorbent is mostly stable under high temperature or pressure. These signify that in comparison to CAC, HMBL is much cheaper and its exploitation for the remediation of EBT-contaminated aqueous solution is quite justified (Table 6).

4. Conclusion

In this research, the potential of HMBL for the abatement of EBT was explored and the following conclusions are made:

- The HMBL has high carbon and low moisture content; active functional groups viz. –OH group, primary amine NH bend, alkyne group CH bend, etc.; rough homogenous sites with uniformly oriented pits and porous structure; high surface area of 825 $m^2\ g^{-1}$; and adsorption average pore diameter of 3.31 nm.
- The maximum removal of EBT is observed to be ~96% at lower concentration (50 mg L^{-1}) and ~60% at higher concentration (500 mg L^{-1}) using 2 g L^{-1} of HMBL at 303 K. However, in the present study, the adsorption experiments are run at C_0 = 200 mg L^{-1} and the optimum adsorbent dose were found to be 2 g L^{-1} for ~92% removal of EBT from aqueous solutions.
- The adsorption process reaches equilibrium in 1 h and after 1.5 h almost became asymptotic with time.
- The optimum temperature of adsorption was 303 K and with the increase in temperature the adsorption of EBT decreases.
- The adsorption of EBT onto HMBL follows pseudo-second-order kinetics.
- Langmuir adsorption isotherm best fitted the experimental findings. The equilibrium adsorption capacity of HMBL for the removal of EBT as calculated from Langmuir isotherm is 133.33 mg g^{-1}.
- The adsorption of EBT onto HMBL is found to be exothermic in nature followed by a decrease in the entropy of the system. The negative value of ΔG° indicates the feasibility and spontaneity of the adsorption process.
- The exhausted EBT-loaded HMBL can be effectively regenerated by 0.1 M NaOH and utilized for three adsorption–desorption cycles without much loss in its adsorption capacity.
- The estimated cost of HMBL are USD 10.684 per kg which is very less compared to CAC.

Thus, HMBL is a potential low-cost alternative to CAC which can effectively treat aqueous solutions contaminated with EBT.

Acknowledgement

The authors are thankful to Director, NIT Silchar for providing laboratory facilities and analysis grant for the present work. The author (Md. Juned K. Ahmed) is thankful to University Grant Commission

(UGC), New Delhi for providing financial assistance under Maulana Azad Junior Research Fellowship (MANJRF) in completion of the research work. The authors are also thankful to anonymous reviewers for their valuable comments in upgrading the quality of the manuscript.

References

[1] H. Zollinger (Ed.), Color Chemistry: Synthesis, Properties and Applications of Organic Dyes and Pigments, second revised ed., VCH, New York, NY, 1991.
[2] N. Barka, M. Abdennouri, M. Makhfouk, Removal of Methylene Blue and Eriochrome Black T from aqueous solutions by biosorption on *Scolymus hispanicus* L.: Kinetics, equilibrium and thermodynamics, J. Taiwan Inst. Chem. Eng. 42 (2011) 320–326.
[3] T. Murugan, A. Ganapathi, R. Valliappan, Removal of dyes from aqueous solution by adsorption on biomass of mango (*Mangifera Indica*) leaves, E-J. Chem. 7 (2010) 669–676.
[4] S. Rangabhashiyam, N. Anu, N. Selvaraju, Sequestration of dye from textile industry wastewater using agricultural waste products as adsorbents, J. Environ. Chem. Eng. 1 (2013) 629–641.
[5] Md.J.K. Ahmed, M. Ahmaruzzaman, R.A. Reza, Lignocellulosic-derived modified agricultural waste: Development, characterisation and implementation in sequestering pyridine from aqueous solutions, J. Colloid Interface Sci. 428 (2014) 222–234.
[6] K. Kadirvelu, M. Kavipriya, C. Karthika, M. Radhika, N. Vennilamani, S. Pattabhi, Utilization of various agricultural wastes for activated carbon preparation and application for the removal of dyes and metal ions from aqueous solutions, Bioresour. Technol. 87 (2003) 129–132.
[7] B.H. Hameed, R.R. Krishni, S.A. Sata, A novel agricultural waste adsorbent for the removal of cationic dye from aqueous solutions, J. Hazard. Mater. 162 (2009) 305–311.
[8] S.S. Kumaar, P.R. Varadarajan, K. Porkodi, C.V. Subbhuraam, Adsorption of methylene blue onto jute fibercarbon: Kinetics and equilibrium studies, J. Colloid Interface Sci. 284 (2005) 78–82.
[9] I.A.W. Tan, B.H. Hameed, W.A.L. Ahmad, Equilibrium and kinetic studies on basic dye adsorption by oil palm fibre activated carbon, Chem. Eng. J. 127 (2007) 111–119.
[10] N. Kannan, M.M. Sundaram, Kinetics and mechanism of removal of methylene blue by adsorption on various carbons—A comparative study, Dyes Pigm. 51 (2001) 25–40.
[11] C. Saka, BET, TG–DTG, FT-IR, SEM, iodine number analysis and preparation of activated carbon from acorn shell by chemical activation with $ZnCl_2$, J. Anal. Appl. Pyrolysis 95 (2012) 19–24.
[12] Ö. Şahin, C. Saka, Preparation and characterization of activated carbon from acorn shell by physical activation with H_2O–CO_2 in two-step pretreatment, Bioresour. Technol. 136 (2013) 163–168.
[13] Ö. Şahin, C. Saka, S. Kutluay, Cold plasma and microwave radiation applications on almond shell surface and its effects on the adsorption of Eriochrome Black T, J. Ind. Eng. Chem. 19 (2013) 1617–1623.
[14] H. Dolasa, O. Sahin, C. Saka, H. Demir, A new method on producing high surface area activated carbon: The effect of salt on the surface area and the pore size distribution of activated carbon prepared from pistachio shell, Chem. Eng. J. 166 (2011) 191–197.
[15] U.V. Ladhe, S.K. Wankhede, V.T. Patil, P.R. Patil, Removal of Erichrome Black T from synthetic wastewater by cotton waste, E-J. Chem. 8 (2011) 803–808.
[16] M. Özdemir, T. Bolgaz, C. Saka, Ö. Şahin, Preparation and characterization of activated carbon from cotton stalks in a two-stage process, J. Anal. Appl. Pyrolysis 92 (2011) 171–175.
[17] V.M. Vucurovic, R.N. Razmovski, U.D. Miljic, V.S. Puskas, Removal of cationic and anionic azo dyes from aqueous solutions by adsorption on maize stem tissue, J. Taiwan Inst. Chem. Eng. 45 (2014) 1700–1708.
[18] U.V. Ladhe, S.K. Wankhede, V.T. Patil, P.R. Patil, Adsorption of Eriochrome Black T from aqueous solutions on activated carbon prepared from mosambi peel, J. Appl. Sci. Environ. Sanit. 6 (2011) 149–154.
[19] U.V. Ladhe, S.K. Wankhede, V.T. Patil, P.R. Patil, Removal of Eriochrome Black T from synthetic wastewater by activated nilgiri leaves, J. Chem. Pharm. Res. 3 (2011) 670–675.
[20] V.K. Gupta, R. Jain, S. Varshney, Removal of Reactofix golden yellow 3 RFN from aqueous solution using wheat husk—An agricultural waste, J. Hazard. Mater. 142 (2007) 443–448.
[21] V.K. Gupta, A. Mittal, L. Kurup, J. Mittal, Adsorption of a hazardous dye, erythrosine, over hen feathers, J. Colloid Interface Sci. 304 (2006) 52–57.
[22] V.K. Gupta, R. Jain, S. Varshney, Electrochemical removal of the hazardous dye Reactofix Red 3 BFN from industrial effluents, J. Colloid Interface Sci. 312 (2007) 292–296.
[23] V.K. Gupta, I. Ali, T.A. Saleh, A. Nayak, S. Agarwal, Chemical treatment technologies for waste-water recycling—An overview, RSC Adv. 2 (2012) 6380–6388.
[24] A. Mittal, J. Mittal, A. Malviya, V.K. Gupta, Removal and recovery of Chrysoidine Y from aqueous solutions by waste materials, J. Colloid Interface Sci. 344 (2010) 497–507.
[25] A. Mittal, L. Kurup, V.K. Gupta, Use of waste materials-bottom ash & deoiled soya, as potential adsorbents for the removal of Amaranth from aqueous solutions, J. Hazard. Mater. 117 (2005) 171–178.
[26] V.K. Gupta, A. Mittal, L. Krishnan, J. Mittal, Adsorption treatment and recovery of the hazardous dye, Brilliant Blue FCF, over bottom ash and de-oiled soya, J. Colloid Interface Sci. 293 (2006) 16–26.
[27] V.K. Gupta, A. Mittal, A. Malviya, J. Mittal, Adsorption of carmoisine A from wastewater using waste materials—Bottom ash and deoiled soya, J. Colloid Interface Sci. 335 (2009) 24–33.
[28] A. Mittal, V.K. Gupta, A. Malviya, J. Mittal, Process development for the batch and bulk removal and recovery of a hazardous, water-soluble azo dye (Metanil Yellow) by adsorption over waste materials (bottom ash and de-oiled soya), J. Hazard. Mater. 151 (2008) 821–832.

[29] A. Mittal, J. Mittal, A. Malviya, D. Kaur, V.K. Gupta, Adsorption of hazardous dye crystal violet from wastewater by waste materials, J. Colloid Interface Sci. 343 (2010) 463–473.
[30] V.K. Gupta, S. Sharma, Removal of zinc from aqueous solutions using bagasse fly ash—A low cost adsorbent, Ind. Eng. Chem. Res. 42 (2003) 6619–6624.
[31] V.K. Gupta, B. Gupta, A. Rastogi, S. Agarwal, A. Nayak, A comparative investigation on adsorption performances of mesoporous activated carbon prepared from waste rubber tire and activated carbon for a hazardous azo dye-Acid Blue 113, J. Hazard. Mater. 186 (2011) 891–901.
[32] V.K. Gupta, I. Ali, V.K. Saini, Defluoridation of wastewaters using waste carbon slurry, Water Res. 41 (2007) 3307–3316.
[33] A.K. Jain, V.K. Gupta, S. Jain, Suhas, Removal of chlorophenols using industrial waste, Environ. Sci. Technol. 38 (2004) 1195–1200.
[34] A.K. Jain, V.K. Gupta, A. Bhatnagar, Suhas, A comparative study of adsorbents prepared from industrial waste for removal of dyes, Sep. Sci. Technol. 38 (2003) 463–481.
[35] V.K. Gupta, A. Rastogi, Biosorption of hexavalent chromium by raw and acid-treated green alga *Oedogoniumhatei* from aqueous solutions, J. Hazard. Mater. 163 (2009) 396–402.
[36] V.K. Gupta, S. Agarwal, T.A. Saleh, Synthesis and characterisation of alumina-coated carbon nano tubes and their applications for lead removal, J. Hazard. Mater. 185 (2011) 17–23.
[37] T.A. Saleh, V.K. Gupta, Column with CNT/magnesium oxide composite for lead (II) removal from water, Environ. Sci. Pollut. Res. 19 (2012) 1224–1228.
[38] V.K. Gupta, R. Jain, A. Mittal, M. Mathur, S. Sikarwar, Photochemical degradation of the hazardous dye Safranin-T using TiO_2 catalyst, J. Colloid Interface Sci. 309 (2007) 464–469.
[39] S. Karthikeyan, V.K. Gupta, R. Boopathy, A. Titus, G. Sekaran, A new approach for the degradation of high concentration of aromatic amine by heterocatalytic Fenton oxidation: Kinetic and spectroscopic studies, J. Mol. Liq. 173 (2012) 153–163.
[40] S. Brunauer, P.H. Emmett, E. Teller, Adsorption of gases in multimolecular layers, J. Am. Chem. Soc. 60 (1938) 309–319.
[41] I. Langmuir, The constitution and fundamental properties of solids and liquids, J. Am. Chem. Soc. 38 (1916) 2221–2295.
[42] H.M.F. Freundlich, Uber die adsorption in losungen (Over the adsorption in solution), Phys. Chem. 57 (1906) 385–471.
[43] C. Tein, Adsorption Calculations and Modelling, Butterworth-Heinemann, Boston, MA, 1994.
[44] B.G. Linsen, Physical and Chemical Aspects of Adsorbents and Catalyst, Academic Press, London, 1970.
[45] J.B. Condon, Surface area and porosity determinations by physisorption, Academic Press, London, 1982.
[46] K.S.W. Sing, D.H. Everett, R.A.W. Haul, L. Moscou, R. Pierotti, J. Rouquerol, T. Siemieniewska, Reporting physisorption of gas/solid systems with special reference to the determination of surface area and porosity, Pure Appl. Chem. 57 (1985) 603–619.
[47] B.C. Lippens, J.H. De Boer, Studies on pore system in catalysis: V. T method, J. Catal. 4 (1965) 319–323.
[48] T. Santhi, S. Manonmani, T. Smitha, K. Mahalaxmi, Adsorption kinetics of cationic dyes from aqueous solution by bioadsorption onto activated carbon prepared from *cucumissativa*, J. Appl. Sci. Environ. Sanit. 4 (2009) 263–271.
[49] R.A. Reza, Md.J.K. Ahmed, A.K. Sil, M. Ahmaruzzaman, A non-conventional adsorbent for the removal of clofibric acid from aqueous phase, Sep. Sci. Technol. 49 (2014) 1592–1603.
[50] M. Ahmaruzzaman, R.A. Reza, Md.J.K. Ahmed, A.K. Sil, Scavenging behavior of *Schumannianthus dichotomus*-derived activated carbon for the removal of methylene blue from aqueous phase, Environ. Prog. Sustainable Energy (in press), doi: 10.1002/ep.11896.
[51] S.A. Khan, R. Rehman, M.A. Khan, Adsorption of Chromium(III), Chromium(VI) and Silver(I) on bentonite, Waste Manage. 15 (1995) 271–282.
[52] D. Murzin, T. Salami, Chemical Kinetics, Elsevier, Amsterdam, 2005.
[53] Md.J.K. Ahmed, M. Ahmaruzzaman, Adsorptive desulfurization of feed diesel using chemically impregnated coconut coir waste, Int. J. Environ. Sci Technol. (in press), doi: 10.1007/s13762-014-0654-4.